# Induction of an Antibody That Catalyzes the Hydrolysis of an Amide Bond

KIM D. JANDA, DIANE SCHLOEDER, STEPHEN J. BENKOVIC, RICHARD A. LERNER

**Catalysis of amide bond hydrolysis is of singular importance in enzymology. An antibody was induced to an analog of a high-energy intermediate anticipated along the reaction coordinate of amide hydrolysis. This antibody is an amidase with high specificity and a large rate enhancement (250,000) relative to the uncatalyzed reaction. This reaction represents the kinetically most difficult hydrolysis reaction yet catalyzed by an antibody.**

ANTIBODIES ARE CAPABLE OF CATALYZING A VARIETY OF chemical transformations (*1–14*). Antigens can be fabricated that structurally resemble high-energy intermediate species anticipated in a chemical reaction, and can then be used to induce antibodies whose binding energy should stabilize such intermediates or transition states along the reaction pathway (*15–18*). For example, the mechanism for the hydrolysis of aryl esters involves the development of a tetrahedral transition state during the process of acyl transfer to water or hydroxide ion (*16–18*). Monoclonal antibodies (abzymes), which have been shown to be highly specific esterases (*2, 3*), were induced by immunizing mice with phosphonate antigens that mimic the stereoelectronic features of the transition states for the hydrolysis of carboxylic esters (*19–22*). Some catalytic antibodies have achieved rate accelerations ($\sim 10^7$) comparable to natural enzymes (*8*), whereas others have displayed remarkable enantioselectivity (*7, 10, 12*). Antibodies have catalyzed the Claisen rearrangement (*9, 10*) and bimolecular (*11, 12*) chemical reactions.

One challenge is to develop catalytic antibodies that can catalyze reactions that are energetically more demanding. The hydrolysis of an amide bond is of prime interest. Amide hydrolysis at slightly alkaline *p*H invovles the intermediacy of a putative zwitterionic tetrahedral species—one of several tetrahedral species interconvertible through rate-limiting proton transfers (Fig. 1) (*16–18*). For an antibody to be an effective amidase, it must have at least bifunctional properties, that is, it must stabilize the oxyanion and must protonate the amide nitrogen for facile expulsion. Despite these complexities, we report the design and synthesis of a hapten that induces an antibody capable of catalyzing amide hydrolysis with large rates and high specificity.

**Immunogen design**. The arylphosphonamidate **1** (Fig. 2) was designed as a mimic of a tetrahedral intermediate anticipated in the hydrolysis of the carboxamide **3**. We synthesized **1** in six steps from the readily available starting materials diethyl 4-aminobenzylphosphonate and *p*-nitroaniline (Fig. 3). Compound **1** displays a tetrahedral and negatively charged phosphorous dioxyanion, along with a possible site for hydrogen bonding to the lone pair of electrons on the nitrogen of the phosphonamidate moiety (*23*). The lone pair of electrons on the nitrogen of the P–N bond of the phosphonamidate may be available for hydrogen bonding, since the P–N bond does not have the same double bond character as the C–N bond of an

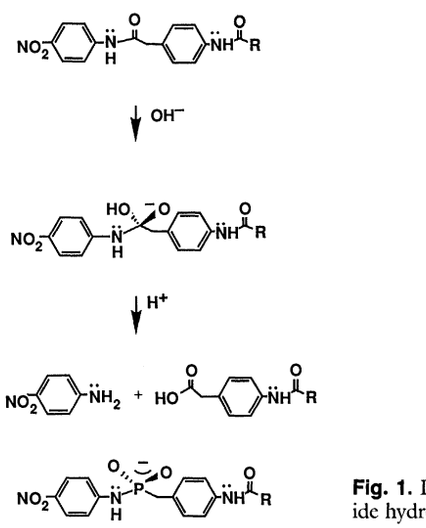

**Fig. 1.** Possible mechanism for amide hydrolysis.

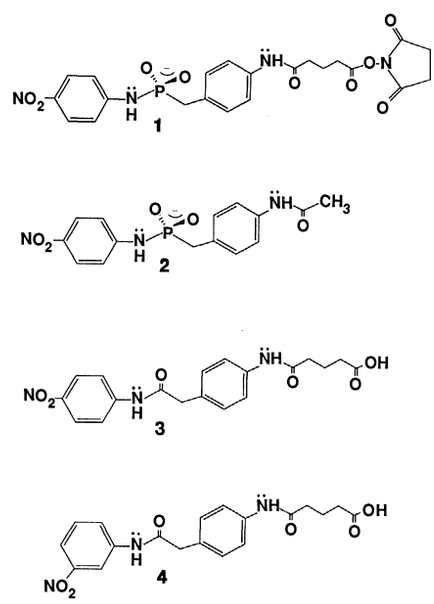

**Fig. 2.** Compounds **1** and **2** represent the phosphonamidates used to induce monoclonal antibody NPN43C9 and inhibit the reaction, respectively. Carboxyamides **3** and **4** act as substrate or inhibitor, respectively, for the reaction catalyzed by NPN-43C9.

K. D. Janda, D. Schloeder, and R. A. Lerner are in the Department of Molecular Biology, Research Institute of Scripps Clinic, La Jolla, CA 92037. S. J. Benkovic is in the Department of Chemistry, Pennsylvania State University, University Park, PA 16802.

amide. Thus the antigen might induce an antibody that has a proton in close proximity to this site that could participate in general acid catalysis. The production of such a structure would be an example of what we have referred to as a "bait and switch" mechanism, in that the antigen has a group or charge that is missing in the substrate, thereby allowing the induced complementary functionality in the antibody to play a different role during catalysis (*13*). Besides having structural and stereoelectronic similarities to the presumed tetrahedral species in amide hydrolysis (Fig. 1), the nitroaniline and benzylic ring systems impart immunogenicity to the compound. The design of hapten **1** also incorporates the heterobifunctional linker appendage (a glutaryl spacer and a *N*-hydroxysuccimide–activated carboxyl) for ease of attachment to carrier proteins, as well as for proper presentation of hapten **1** to the immune system (*2, 3*).

**Induction of antibodies**. A keyhole limpet hemocyanin (KLH)–phosphonamidate **1** conjugate was used to immunize 129GIX$^+$ mice for the production of monoclonal antibodies (*24, 25*). From this immunization, 44 monoclonal antibodies were selected for their ability to bind in an enzyme-linked immunosorbent assay (ELISA) (*26*) to **1** conjugated to bovine serum albumin (BSA) (*27*). All 44 cloned myeloma cell lines were separately injected into mice for generation of ascites fluids, from which antibody was purified by salt precipitation followed by anion exchange chromatography. The individual monoclonal antibodies were screened for amide hydrolysis by using **3** as a substrate. On the basis of activity one (NPN43C9) was selected for further study.

We purified NPN43C9 by saturated ammonium sulfate (SAS) precipitation and by affinity and anion exchange chromatography (Fig. 4). The isolated immunoglobulin G (IgG) fraction was subjected to enzyme digestion followed by anion exchange chromatography to yield a highly purified Fab fragment (Fig. 4). As controls, antibodies that appeared to have binding but not catalytic activity were purified in an identical fashion. A study of the effect of *p*H and salt concentration on the catalytic activity showed maximum activity at *p*H 9.0 and almost complete inhibition in the presence of 150 m*M* NaCl (*28, 29*). Thus kinetic studies were carried out in 50 m*M* 2-cyclohexylaminoethane sulfonic acid (CHES) buffer, 80 μ*M* NaCl, *p*H 9.0.

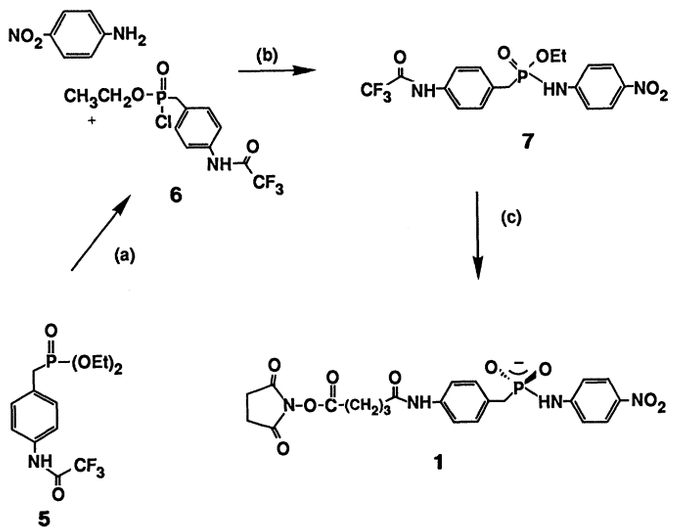


**Fig. 3.** Synthesis of **1**. (a) **5** was converted to **6** in the presence of $PCl_5$ in $CHCl_3$ at 40°C for 2 hours. (b) **6** and *p*-nitroaniline were condensed in the presence of potassium-*tert*-butoxide in DMSO at room temperature for 24 hours. (c) The product **7** was reduced with $NaBH_4$ and ethanol, and then derivitized with $ClCO(CH_2)_3COON(COCH_2)_2$ in the presence of $CH_2Cl_2$ and $(CH_3)_3N$, and then reacted with trimethylsilyl bromide at 45°C in $CH_3CN$.

**Kinetic analysis and abzyme specificity**. The initial rates of hydrolysis measured as of function of substrate **3** concentrations followed Michaelis-Menten kinetics, consistent with Eq. 1 ($K_m$ is the Michaelis constant) and Fig. 5 (see Table 1).

$$\begin{array}{ccc} \text{NPN43C9} + \mathbf{3} & \xrightarrow{k_{uncat}} & \text{products} \\ \uparrow\downarrow K_m & & \\ \text{NPN43C9} \cdot \mathbf{3} & \xrightarrow{k_{cat}} & \text{NPN43C9} + \text{products} \end{array} \quad (1)$$

Comparison of the $k_{cat}/k_{uncat}$ gives a rate acceleration for hydrolysis of **3** of approximately 250,000. The Fab fragment of NPN43C9 had approximately the same $K_m$ and maximal rate $V_{max}$ as the intact IgG molecule, whereas several control IgG molecules that bound to **1**, when purified in the same way, were not catalytic.

To establish the specificity of NPN43C9, we studied the rates of hydrolysis of substrates modified in their acyl or aniline portions. A variety of amino acid *p*-nitroanilides [L-leucine, *N*-α-benzyl-DL-arginine, L-lysine, L-proline, *N*-glutaryl-L-phenylalanine, *N*-CBz-glycyl-glycyl-L-leucine (CBz, carboxybenzyl), Glu-Phe-Leu, *S*-benzyl-L-cysteine, L-valine, *N*-α-CBz-L-arginine, acetyl-L-asparagine, and *N*-benzoyl-L-tyrosine] were not substrates for NPN43C9 (*30*). Substitution of *m*-nitroaniline or *o*-nitroaniline for the *p*-nitroaniline

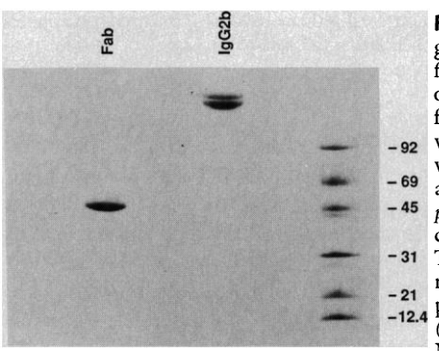


**Fig. 4.** SDS–polyacrylamide gel electrophoresis of purified IgG and Fab fragment of NPN43C9. The globulin fraction from ascitic fluid was precipitated by dropwise addition of saturated ammonium sulfate at 4°C, *p*H 7.2, to achieve a final concentration of 45 percent. The ammonium sulfate was removed by dialysis against phosphate-buffered saline (0.01*M* $Na_3PO_4$, 0.15*M* NaCl, *p*H 7.0). The concentrated globulin was affinity-purified on a protein G–Sepharose column. The antibody was loaded onto a protein G–Sepharose column and nonadherent material was removed by extensive washing (20 to 30 column volumes) with 0.1*M* phosphate buffer, *p*H 7.0. The adherent antibody was eluted with 0.05*M* citric acid, *p*H 3.0, and immediately neutralized by collecting the active fractions into 1*M* tris, *p*H 9.0. The affinity-purified antibody was dialyzed into 75 m*M* tris buffer, *p*H 8.0, and further purified by anion-exchange chromatography on a monoQ (fast protein liquid chromatography, FPLC) column. The antibody was eluted from the monoQ column by a linear salt gradient, and peak fractions were pooled and concentrated for further study. The antibody purified by the above procedure was judged to be homogeneous by gel electrophoresis. The two closely spaced bands were separated by further anion-exchange chromatography, and each had comparable antigen-binding activity, suggesting that the slightly different mobility in gel electrophoresis was due to post-translational modification, presumably differential glycosylation of the Fc portion of the molecule (see below). To prepare the Fab fragment, ~40 mg of IgG purified as above was diluted into 0.1*M* sodium acetate buffer, *p*H 5.5, containing 3 m*M* EDTA. Predigested papain (800 μg) was added to the IgG solution, and the mixture was incubated at 37°C for 2 hours. The reaction was terminated by addition of iodoacetamide to a final concentration of 30 m*M*. The Fab was further purified by anion exchange chromatography. The digest was dialyzed against 20 m*M* tris, *p*H 7.8, and the Fab fraction separated from other components of the digestion mixture by DEAE-cellulose anion-exchange chromatography on a Memsep 1000 cartridge column. The Fab fragment was judged to be homologous by gel electrophoresis. The absence of two bands in the Fab fragment further suggests differential glycosylation of the Fc portion of the intact IgG.

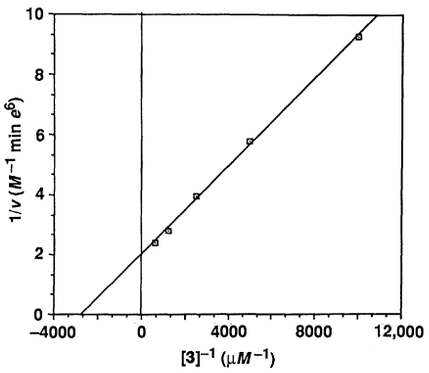


**Fig. 5.** Lineweaver-Burke plot for amide hydrolysis of substrate **3** by NPN43C9. Rates were determined as described in Table 1.

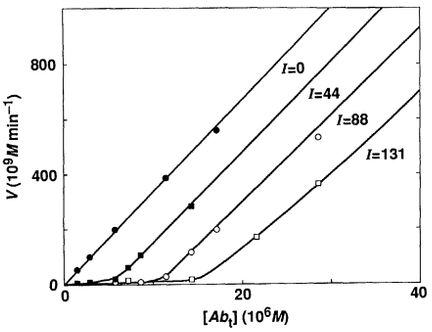


**Fig. 6.** Plot of steady-state velocity ($v$) as a function of total antibody concentration ($Ab_t$) in the absence and in the presence of different concentrations of reversible tight-binding inhibitor. The figures adjacent to each curve represent the total concentrations ($\mu M$) of inhibitor **2**. Each set of data was obtained at a constant substrate concentration of 1600 ($\mu M$). The apparent $K_i$'s and number of antibody binding sites were then determined by varying the concentration of substrate **3** (400 to 1600 $\mu M$) at a fixed concentration of inhibitor **2** (87 $\mu M$) and then fitting the data to Eq. 2.

leaving group of **3** rendered these compounds nonsubstrates (*31*). This substrate specificity is similar to that seen with other catalytic antibodies (*2, 3, 8*), and presumably reflects the well-known sensitivity of antibody binding to structural isomerism in the nitrophenyl ring (*32*).

Basic inhibition studies were performed with phosphonamidate **2** as the inhibitor. Since in antibody catalysis the inducing antigen and inhibitor are either the same or structurally similar, a high degree of complementarity between the antibody and the inhibitor can be expected that leads to tight binding (*33*). Moreover, since catalytic antibodies may have relatively low turnover numbers, antibody concentrations are generally used that are comparable to those of the inhibitor. Tight-binding inhibition was confirmed by plots of steady-state velocity ($v$) as a function of total antibody concentration ($Ab_t$), in which the presence of different concentrations of inhibitor **2** generated classical concave-upward curves (Fig. 6) (*33*). The $K_i$ and $Ab_t$ concentrations were determined according to the method of Blanchard and Cleland (*34*), in which the tight-binding inhibition data were fit to Eq. 2, which corrects for depletion of the initial inhibitor concentrations by binding to the abzyme:

$$\log v = (V/2)\{AE - I - K + [(K + AE - I)^2 + 4KI]^{1/2}\} \quad (2)$$

where $A$ is the concentration of active sites, $E$ is the volume of enzyme solution added, $I$ is the concentration of inhibitor **2**, and $K$ is the inhibition constant for **2**.

The time course for product formation when the reaction was initiated by either the addition of substrate after preincubation of the abzyme with inhibitor or the addition of the abzyme were both linear and proceeded at the same rate. Thus the inhibition is reversible and the above equation is applicable.

**Table 1.** Kinetic parameters for hydrolysis of amide **3** by NPN43C9. Velocities were determined spectrophotometrically by measuring the initial linear absorbance change at 404 nm (release of *p*-nitroaniline). The antibody [10 $\mu M$ (Figs. 5 and 6) and 8 $\mu M$ (Fig. 7), average value determined from a bicinchoninic acid (BCA) assay and absorbance at 280 nm, assuming a molecular weight of 160,000 for IgG] was preincubated at 37°C (CHES, *p*H 9.0, 0.08 m$M$ NaCl) and reactions were initiated by addition of varying aliquots of a 50 and 100 m$M$ stock solution of amide **3** in DMF to give a substrate concentration of 100 to 1600 $\mu M$. An alternative cosolvent system of 0.2 to 2.4 percent dimethyl sulfoxide (DMSO) plus acetonitrile to make 5 percent organic phase could be used to solubilize substrate **3**. This solvent system gives some differences in kinetic parameters, but has the advantage that the microprecipitate that occurs when DMF is added to some IgG preparations is avoided. Because of the relatively slow rate of reaction, the first-order rate constant ($k_{uncat} = 3.36 \times 10^{-7}$ min$^{-1}$) for the hydrolysis in the absence of antibody was measured by high-performance liquid chromatography (HPLC; RP-C18, $CH_3CN$-$H_2O$, isocratic 21/79). The *p*-nitroaniline product in the presence of NPN43C9 was also confirmed with these HPLC conditions. Initial spectrophotometric rates stand uncorrected, as the background rate of hydrolysis did not contribute to the antibody-catalyzed rate under typical assay conditions. The error in the kinetic parameters is ±5 percent (SEM).

| Cosolvent | $K_m$ ($10^{-6}M$) | $V_{max}$ ($10^{-7}M$ min$^{-1}$) | $k_{cat}$ (min$^{-1}$) | $k_{cat}/k_{uncat}$ ($10^5$) |
|---|---|---|---|---|
| DMF | 370 | 5.0 | 0.05 | 1.5 |
| DMSO-$CH_3CN$ | 562 | 4.2 | 0.08 | 2.5 |

The nature of the inhibition was determined by replotting the apparent $K_i$ as a function of substrate concentration. This analysis showed that phosphonamidate **2** was a mixed inhibitor of the reaction of NPN43C9 with amide substrate **3**, varying as a hyperbolic function of the concentration of **3**. At low substrate concentration, the inhibition constant $K_{is}$ = 10 $\mu M$ (associated with inhibitor binding to free abzyme); at infinite substrate concentration, $K_{ii}$ = 2.5 $\mu M$ (associated with inhibitor binding to the abzyme **1** complex) (*35*). The calculated maximum number of enzyme binding sites was 5.1 (SE ± 0.9). Immunoglobulin G antibodies are expected to exhibit a total of two binding sites and thus two to three additional binding sites were detected with inhibitor **2**.

Additional binding sites that alter abzyme turnover ($k_{cat}$ in Eq. 1) would give rise to the appearance of noncompetitive inhibition. Their loci are secondary sites in the complementarity determining regions (CDRs) of the antibody, as has been observed by x-ray diffraction studies to occur with small aryl compounds, such as vitamin K, riboflavin, and nitrophenolates, that bind tightly to the CDRs of some randomly selected myeloma and hybridoma antibodies, as well as immunoglobin light-chain dimers (*36*). In contrast, the less charged *m*-nitroanilide **4** was a purely competitive inhibitor of the reaction of NPN43C9 with the amide substrate **3**, and exhibited a $K_i$ of 804 $\mu M$ (Fig. 7). Thus the high specificity of antibody catalysis is manifest in that, despite the near equivalence in binding, **3** is a substrate and **4** an inhibitor of the reaction (*37*). Moreover, this observation, coupled with the quantitative aspects of inhibition by **2**, the unaltered steady-state parameters for catalysis by the Fab fragment, and the high purity of the abzyme preparation (Fig. 4), all identify NPN43C9 as the catalyst for the hydrolysis of **3**.

**Mechanistic considerations**. The large rate enhancement of $10^5$ for the antibody-catalyzed reaction relative to its solution counterpart cannot be simply rationalized without invoking chemical mechanisms for catalysis based on the presumption that the difference between the binding of **2** ($K_i$) and **3** ($K_m$) to the antibody is an index of the available transition state binding energy [$\Delta\Delta G‡ = -2.2$ kcal mol$^{-1}$ (*38*)]. A triple mutant of the enzyme subtilisin, in which each amino acid of the catalytic triad of His, Ser, and Asp is replaced

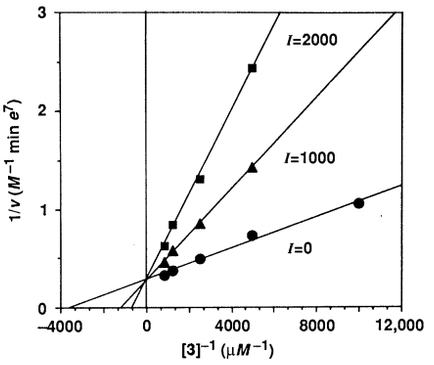


**Fig. 7.** Lineweaver-Burke plot for hydrolysis of substrate **3** by the NPN43C9. Velocities were determined as described in Table 1; (●), no inhibitor present; (▲), inhibited by 1000 μ*M* *m*-nitro derivative **4**; (■) inhibited by 2000 μ*M* *m*-nitro derivative **4**.

by an Ala residue, hydrolyzes a *p*-nitroanilide peptide substrate 3000-fold more rapidly than the corresponding uncatalyzed reaction, which gives an estimate of the extent of catalysis that can be achieved by stabilization of the transition state by binding determinants other than the catalytic triad (*39*). However, the rate enhancement observed for NPN43C9 is ~50-fold greater than that observed for the subtilisin mutant, suggesting that factors other than transition state stabilization, such as functioning acid or base residues or ground-state destabilization, are involved in the catalysis. Participation of acid-base catalysis is also anticipated on mechanistic grounds, since the hydrolysis of substituted acetanilides at mildly alkaline *p*H is thought to require expulsion of aniline rather than its highly basic anion (*40, 41*). The sensitivity of $k_{cat}$ to salt may reflect specific anion binding or effects on the $pK_a$ of essential binding site residues (*16*). Because the hydrolysis of substituted acetanilides is relatively insensitive to substituents ($\rho = 0.1$) (*40*), the lack of abzyme-assisted hydrolysis for the *m*-nitroanilide **4** is probably a manifestation of unproductive binding, rather than a $pK_a$ effect on $k_{cat}$, if we assume that the mechanism and rate-limiting step are the same in the enzymic and nonenzymic reactions.

Since the induction of the first catalytic antibodies, catalysis of a succession of energetically more demanding acyl transfer reactions with respect to increased $pK_a$ of the leaving group has been achieved, and now includes amide bond hydrolysis. The understanding gained from such studies should be useful in meeting the next important challenge in abzyme catalysis, namely, the hydrolysis of alkyl amides, which include peptides and proteins.

## REFERENCES AND NOTES


1. R. A. Lerner, in *Proceedings of the XVIIIth Solvay Conference on Chemistry*, G. Van Binst, Ed. (Springer-Verlag, Berlin, 1983), pp. 43–49.
2. A. Tramontano, K. D. Janda, R. A. Lerner, *Proc. Natl. Acad. Sci.* U.S.A. **83**, 6736 (1986).
3. ———, *Science* **234**, 1566 (1986).
4. R. A. Lerner and A. Tramontano, *Trends Biochem. Sci.* **12**, 427 (1987).
5. S. J. Pollack, J. W. Jacobs, P. G. Schultz, *Science* **234**, 1570 (1986).
6. J. Jacobs, P. G. Schultz, R. Sugasawara, M. Powell, *J. Am. Chem. Soc.* **109**, 2174 (1987).
7. A. D. Napper, S. J. Benkovic, A. Tramontano, R. A. Lerner, *Science* **237**, 1041 (1987).
8. A. Tramontano, A. A. Ammann, R. A. Lerner, *J. Am. Chem. Soc.* **110**, 2282 (1988).
9. D. Hilvert, S. H. Carpenter, K. D. Nared, M. T. M. Auditor, *Proc. Natl. Acad. Sci.* U.S.A. **85**, 4953 (1988); D. Y. Jackson *et al.*, *J. Am. Chem. Soc.* **110**, 4841 (1988).
10. D. Hilvert and K. D. Nared, *J. Am. Chem. Soc.*, **110**, 5593 (1988).
11. K. D. Janda, R. A. Lerner, A. Tramontano, *ibid.*, p. 4835.
12. S. J. Benkovic, A. D. Napper, R. A. Lerner, *Proc. Natl. Acad. Sci. U.S.A.* **85**, 5355 (1988).
13. R. A. Lerner and S. J. Benkovic, *Bioassays*, in press.
14. A. Tramontano, K. Janda, A. D. Napper, S. J. Benkovic, R. A. Lerner, *Cold Spring Harbor Symp. Quant. Biol.* **52**, 91 (1987).
15. L. Pauling, *Am. Sci.* **36**, 51 (1948).
16. W. P. Jencks, *Catalysis in Chemistry and Enzymology* (McGraw-Hill, New York, 1969), pp. 354–355 and 524–525; *Chem. Rev.* **72**, 705 (1972); A. C. Satterthwait and W. P. Jencks, *J. Am. Chem. Soc.* **96**, 7019 (1974); J. C. Fishbein, H. Baum, M. M. Cox, W. P. Jencks, *ibid.* **109**, 5790 (1987).
17. A. Fersht, Ed., *Enzyme Structure and Mechanism* (Freeman, New York, 1985).
18. T. C. Bruice and S. J. Benkovic, *Bioorganic Mechanisms* (Benjamin, New York, 1966), chap. 1.
19. R. Wolfenden, *Acc. Chem. Res.* **5**, 10 (1972).
20. G. E. Lienhard, *Science* **180**, 149 (1973).
21. P. A. Bartlett and C. K. Marlowe, *Biochemistry* **22**, 4618 (1983).
22. R. E. Galardy, *ibid.*, p. 1990.
23. T. A. Modro, *ACS Symp. Ser.* **171**, 619 (1981).
24. G. Kohler and C. Milstein, *Nature* **256**, 495 (1975).
25. The conjugate was prepared by slowly adding 2.5 mg of **1** in 250 μl of dimethyl formamide (DMF) to 2 mg of KLH in 750 μl of 0.01*M* sodium phosphate buffer, *p*H 7.2, while stirring at 4°C for 1 hour. Four 8-week-old mice each received an intraperitoneal (IP) injection of 100 μg of **1** conjugated to KLH and emulsified in complete Freund's adjuvant, followed by an IP injection of 50 μg of the **1**-KLH conjugate in alum 2 weeks later. One month after the second injection, the mouse with the highest antibody titer to **1** (25,600) was injected intravenously with 50 μg of the **1**-KLH conjugate; 3 days later the spleen was taken for the preparation of hybridomas. Spleen cells ($1.0 \times 10^8$) were fused with $2.0 \times 10^7$ SP2/O myeloma cells. Cells were plated into 45 96-well plates; each well contained 150 μl of hypoxanthine, aminopterin, thymidine–Dulbecco's minimal essential medium (HAT-DMEM) containing 1% nutridoma and 2% BSA.
26. E. Engvall, *Methods Enzymol.* **70**, 419 (1980).
27. After 2 or 3 weeks, the antibodies produced by wells containing macroscopic colonies were assayed by ELISA for binding to **1**. Colonies that initially produced antibodies that bound to **1** were subcloned twice, after which 44 remained active. The subtype distribution of the 44 monoclonal antibodies was 27 IgGγ1, 11 IgG2a, 5 IgG2b, and 1 IgG3. All 44 monoclonal antibodies were injected into pristane-primed BALB/c × 129GIX$^+$ mice to generate ascitic fluid. For initial studies, IgG was purified from the ascitic fluid by salt precipitate and anion exchange chromatography. Each purified monoclonal antibody was dialyzed into three different buffers [50 m*M* 2-(*N*-morpholino)ethanesulfonic acid (Mes), *p*H 5.5; 50 m*M* phosphate-buffered saline, *p*H 7.2; and 50 m*M* CHES, *p*H 9.0] and assayed for their ability to hydrolyze **3**. Antibody (250 μl) from a stock solution of 10 m*M* was incubated at 37°C with 12 μl of a stock solution of 40 m*M* **3** in a 96-well microtiter plate, and the absorbance at 405 n*M* was monitored.
28. Antibody NPN43C9 is characteristic of many IgG2b monoclonal antibodies, which are euglobulin-like proteins that precipitate at 4°C from solutions of low ionic strength (*29*). To avoid this, the antibody was stored at 4°C in buffer containing 150 m*M* NaCl, which was removed immediately prior to use by dialysis against 50 m*M* CHES, 80 μ*M* NaCl, *p*H 9.0, at 22°C.
29. J. W. Goding, *Monoclonal Antibodies: Principles and Practice* (Academic Press, New York, 1986).
30. Reactions were carried out in a microtiter-well assay in 5 percent DMF, 50 m*M* CHES, *p*H 9.0, and followed for the release of *p*-nitroaniline in a kinetic plate reader at 405 nm for 48 hours. The detection limit of this system is estimated to be 25 μ*M* *p*-nitroaniline.
31. Velocities were determined spectrophotometrically by measuring the initial linear absorbance change at 400 nm (release of *o*- or *m*-nitroaniline).
32. K. Landsteiner, *The Specificity of Serological Reactions* (Thomas, Springfield, IL, 1936); A. Nisonoff and D. Pressman, *J. Am. Chem. Soc.* **79**, 1616 (1957).
33. J. W. Williams and J. F. Morrison, *Methods Enzymol.* **63**, 437 (1979).
34. J. S. Blanchard and W. W. Cleland, *Biochemistry* **19**, 3543 (1980).
35. The terms $K_{is}$ and $K_{ii}$ denote inhibition constants derived from the slopes and intercepts of double reciprocal plots of velocity versus substrate concentration at varying inhibitor levels.
36. A. B. Edmundson, K. R. Ely, J. N. Herron, *Mol. Immunol.* **21**, 561 (1984); A. B. Edmundson and K. R. Ely, *ibid.* **22**, 463 (1985); *Ciba Found. Symp.* **119**, 107 (1986); A. L. Gibson *et al.*, *Mol. Immunol.* **22**, 499 (1985); D. M. Segal *et al.*, *Proc. Natl. Acad. Sci. U.S.A.* **71**, 4298 (1974); L. M. Amzel, R. J. Poljak, F. Saul, J. M. Varga, F. F. Richards, *ibid.*, p. 1427; M. Potter, *Adv. Immunol.* **25**, 141 (1977).
37. It is reasonable to presume that $K_i$ and $K_m$ are true dissociation constants.
38. The rate acceleration due to transition state stabilization may be given by:

$$K_a/K_t = k_{ab}/k_n$$

where $K_a$ and $K_t$ are the binding constants for the substrate and transition state, respectively, and $k_{ab}$ and $k_n$ are the rate constants for the antibody-catalyzed and antibody-uncatalyzed reaction (*12*). $K_a$ and $K_t$ are approximated by $K_m$ and the inhibition constant, $K_i$, giving a ratio of 37 $[(370 \times 10^{-6})/(10.0 \times 10^{-6})]$, which would suggest a rate acceleration of less than 100.
39. P. Carter and J. A. Wells, *Nature* **332**, 564 (1988).
40. M. L. Bender and R. J. Thomas *J. Am. Chem. Soc.* **83**, 4183 (1961).
41. R. M. Pollack and M. L. Bender, *ibid.* **92**, 7180 (1970); At millimolar hydroxide levels, the alkaline hydrolysis may proceed with expulsion of the *p*-nitroaniline anion.



42. We thank A. Satterthwait and C. E. Grimshaw for many helpful discussions and use of computer programs for calculation of kinetic parameters, D. A. McLeod and S. Boross for excellent technical assistance, and P. Wirsching for his valuable suggestions. K.D.J. gratefully acknowledges IGEN Inc. for financial support.

20 July 1988; accepted 29 July 1988